SIDE LOAD EFFECT ON TURBOMACHINES WITH AMB

Agahi, R. R., Ershaghi, B. B.
Leonhard, M. and Ispas, I.
ACT Division of Atlas Copco

ABSTRACT

Turbomachinery bearing systems are normally designed for radial loads corresponding to the weight of the rotor. Non-uniform pressure distribution around the wheel(s) of a turbomachine may also contribute to the magnitude of gas dynamic radial load, called side load. Conventional oil bearings have such a comfortable margin of load capacity that dynamic load is not of any design significance.

Active Magnetic Bearing (AMB) systems have limited load capabilities. Turbomachinery manufacturers have developed their own methods of calculating side load. When the magnitude of side load exceeds the AMB's capacity, several corrective actions are available.

AMB applications for off-shore platforms or dew point control of natural gas using turboexpanders are on the rise. Process gas pressures of these applications are in the range of 60-100 Bar and the side load effect is significant for high density process gas or liquid if turbomachine components are not designed correctly. Therefore, it is essential to use Computational Fluid Dynamic (CFD) to calculate the flow field in the casings. Corrective action should not sacrifice turbomachine performance which may result in a less desirable market for AMB.

In this paper, the authors present one method of side load calculation and its theoretical background. In conclusion, the merits of alternative solutions are discussed.

INTRODUCTION

Active Magnetic Bearing (AMB) load capabilities, both radially and axially, are much less than conventional oil bearings. The radial load limitation is mostly due to the limited magnetic flux density of the materials used. The axial load restriction is, for the most part, governed by the mechanical limitations of the thrust disk. At the present time the limit for radial unit loading is 0.5 N/mm^2 compared to the 3.5 N/mm^2 for hydrodynamic oil bearings. The limit for axial loading is 0.3 N/mm^2 and 2.0 N/mm^2 for the AMB and the conventional oil bearing respectively.

Therefore, the size of an AMB has to be much larger than the conventional oil bearing for a given radial load. However, mechanical constraints do not allow the AMB physical size to be sufficiently enlarged to carry the radial and/or axial load equivalent of the conventional oil bearing.

The first installations of turboexpander-compressors with AMB's experienced problems due to excessive radial and/or axial load. While the source of excessive axial loads was known to be process upsets, the cause of additional radial loads was not that obvious. Further evaluation revealed that gas dynamic radial loading was the cause of these failures. Gas dynamic radial loads are not significant in conventional oil bearings, due to the higher unit load capability of oil bearings with respect to AMB's.

In this paper, the authors explain how gas dynamic radial load develops in an expander or compressor. Then a simulation model is constructed and validation of this model is performed by comparing the output of other known approaches with the model. Process induced side loads as a result of pressure fluctuations are considered. Alternative remedies to counter the gas dynamics and/or process induced side loads are discussed together with methods of analysis.

Gas Dynamic Radial Load

The source of gas dynamic radial loads on the compressor wheel are different to those at the expander wheel. In the following sections, we explore how the gas dynamic radial loads may be developed.

Compressor Gas Dynamic Radial Load

In a compressor with vaneless diffuser followed by a dump casing, the nonuniform, circumferential flow resistance across the diffuser walls induces an asymmetric gas pressure around the wheel. Nonuniform peripheral gas pressure results in unbalanced loading on the wheel and hence a radial bearing load (Figure 8).

Expander Gas Dynamics Radial Load

On the expander side, the expander wheel is surrounded by the nozzle vanes. The nozzle vanes, in turn, receive gas from a torus space which is connected to the expander inlet piping. Any nonuniformity in the torus space and/or in the nozzle vane design may result in a nonuniform pressure distribution around the expander wheel. Nonuniform gas pressure around the expander wheel will result in a nonuniform load and hence produce a gas dynamic radial load on the expander and bearing. In the expander case, however, the nozzle throat flow resistance is much larger than the casing peripheral pressure nonuniformity. The latter acts as a buffer and hence the expander wheel circumferential pressure variation is smaller than that of the compressor side. This smaller pressure variation will produce much less radial load when compared to the compressor case.

Analysis of Gas Dynamic Radial Load

To evaluate gas dynamic radial loads, Computational Fluid Dynamics (CFD) are

used. This method is based on the potential theory that was developed by the National Aeronautics and Space Administration (NASA) in the early eighties. In the CFD approach, the equation of motion for the real fluid is developed from a finite element of the fluid [1]. As the initial step in our modeling, we construct a large external boundary connected to the casing under study. This boundary is configured at the expander inlet or at the compressor discharge. Figure 1 shows a cross section of an expander-compressor with magnetic bearings. From this point on, analysis for an expander or a compressor is the same. Figure 2 shows the large boundary for the compressor discharge. In this graphical representation, the wheel is shown as a small circle in the center (broken line). We continue this work with the compressor side analysis.

Analysis of Gas Dynamic Radial Load for a Compressor

The compressor in Figure 2 may be mapped into polar coordinates. Figure 3 is the result of such mapping with the following characteristics:

- Compressor wheel is transformed into a straight, broken line.
- Casing inner surface is transformed into a straight line, identified by the squares
- Casing outer surface, including the discharge neck and flange, is transformed into a loaf-like body identified by triangles and circles

The above mapping, Figure 3, is then repeated every 360°. The outcome of this repetition is the mapping of the compressor casing as an infinitely cascaded system, similar to what is shown in Figure 4 for two such repetitions. It is obvious that in our analysis, we have assumed that the center of the wheel is equivalent to the point source for compressor flow. This point source is mapped into a straight line at the radius ratios of zero as shown in Figure 4.

The next step in this simulation modeling is to model the streamtubes. By definition, a streamtube is an equivalent tubular cross section of the actual flow channel. Figure 5 represents the equivalent cascade streamtube thickness distribution as a function of radius. The small streamtube thickness for a radius less than 0.735 represents the diffuser area. The streamtube thickness of the compressor concentric casing between the diffuser and the compressor discharge neck and that of the discharge neck to the compressor discharge flange is shown between radii of 0.735 and 1.000. The constant streamtube thickness above a radius of 1.000 approximates the compressor discharge piping.

Description of the Results:

The first gas dynamic variable that is evaluated is the gas velocity at the discharge of the compressor wheel. As shown in Figure 6, radial velocity at the discharge of the wheel is nonuniform and the magnitude of variation is a function of rotational speed (actual volumetric flow). The higher the rotational speed, the larger the magnitude of radial velocity fluctua-

tion. As shown in Figure 7, variation of the total velocity has the same pattern as the radial velocity variation but with a minor phase shift.

It is obvious that a nonuniform radial/total velocity in the compressor wheel discharge area will result in a nonuniform static pressure in this area. Variation of the compressor wheel discharge static pressure is shown in Figure 8. The pattern of variation for static pressure is similar to that of radial velocity, i.e. static pressure variation increases as rotational speed is increased. This nonuniform static pressure distribution around the compressor wheel produces a net radial load on the wheel and hence on the compressor side bearing. The resultant net radial load is shown in Figure 9. Since variation of static pressure is a function of volumetric flow (or RPM), Figure 9 shows both the load and volumetric flow normalized for rotational speed, RPM.

It is interesting to note that the direction of the net gas dynamic radial load is opposite to the gravitational force due to rotor weight. Figure 10 shows radial thrust direction over the range of volumetric flow.

Validation of the Simulation Model

Although simulation modeling by CFD normally produces reliable results, validation of the model is an essential part of any simulation. To validate the CFD model developed above, we compared the simulation results to the calculated values by Stepannof [2] and Biheller [3] prediction approaches. This comparison is shown in Figure 11. Although the numerical values are different from point to point, the general trend over compressor inlet volumetric flow is evident. It is interesting to note that the emphasis of the models is different in each case. The Stepannof approach emphasizes the compressor's overall headrise. The Biheller method stresses the compressor wheel tip speed. The CFD model considers all the variables in a more complex and detailed fashion. Therefore, one would expect that the latter model will produce more accurate results when compared to the first two models.

One last observation in this comparison is that the orientation of the net radial load that is
-140° by Stepannof's, is predicted to be -90° by both Biheller's and CFD's.

Process Induced Fluctuations

In the previous sections, we showed that the gas dynamic side load is an inherent phenomenon in turboexpander-compressors. Unfortunately, when a turboexpander-compressor is utilized in a natural gas processing plant for dew point control, for example, the process is not normally stable and the turboexpander is exposed to process induced fluctuations.

Process induced fluctuations make a turboexpander compressor with magnetic bearings even more susceptible to excessive side loads. While the Stepannof approach and Biheller method are not flexible enough to consider process fluctuations,

the proposed CFD simulation model is.

To demonstrate the proposed methodology, we assume that the compressor discharge process is disturbed by a sinusoidally shaped fluctuation with an amplitude of $\pm$ 3 Bars. Since we are concerned with one cycle, frequency of the perturbation is not relevant to this analysis.

Process Induced Radial Side Load

The process induced 3 bar fluctuation pressure pulse at the compressor discharge is assumed to have 5 to 10 hz frequency and results in compressor flow oscillations. Since the fluctuation frequency is low, the acoustic effect is very small. Therefore, it is relevant to assume quasi-steady flow and based on this we can proceed with the study of unsteady radial load prediction.

The compressor performance curve (Figure 12) provides the slope of pressure rise versus flow rate. This characteristic can be interpreted for any finite compressor pressure change and will induce equivalent flow rate variations as long as the compressor inlet pressure is held constant.

The steady state radial load and flow relationship curve (Figure 9), may be combined with the compressor steady state performance curve to predict the compressor unsteady radial load due to pressure pulsation at the compressor discharge.

Assuming compressor steady state flow rate, speed, and pressure rise are Q, N, and H, respectively, the following procedure outlines the methodology of unsteady radial load prediction:

- At a given steady state compressor operating condition using Figure 12, find the flow rates Q+ and Q- corresponding to H+1.5 bars, and H-1.5 bars, for the design rotational speed.

- With reference to Figure 9, use Q-, Q, and Q+ to predict the radial loads T-, T, and T+ respectively. The steady state radial load value is T. The fluctuation maximum and minimum radial loads are T+ and T- respectively.

The steady and unsteady radial load predictions for two typical compressors under steady state operation (two flow conditions) are summarized in Table I.

Protection Against Gas Dynamics Radial Load

Protection against gas dynamics radial load is achieved by introducing a buffer, or non-reflecting channel, between the wheel discharge and the compressor casing. This may be achieved either by installation of compressor discharge guide vanes (DGV) or reshaping the compressor wheel discharge diffuser gap.

DGV design requires special attention to ensure that compressor performance is not compromised. Increasing the diffuser gap, for example, may reduce the surge margin. Therefore, gas dynamic side load

reduction alternatives have to be chosen with the compressor process condition in mind.

Conclusion

Active Magnetic Bearing systems have limited axial and radial load capabilities. Turbomachines with active magnetic bearings are utilized in high density natural gas applications. In such applications, the active magnetic bearings are subject to gas dynamic and process induced radial loads. Total radial load may exceed the bearing's capacity. Gas dynamic and process induced side load are predictable and should be evaluated at the design stage. Computational fluid dynamic methods are the most promising prediction approach. When radial load exceeds the magnetic bearing's capacity, the most effective measures to reduce gas dynamic and process induced side loads are to be considered.

REFERENCES

1. E.R. McFarland, A Rapid Blade-to-Blade Solution for Use in Turbomachinery, NASA TM-83010, NASA Lewis Research Center, March 1983.

2. A.J. Stepannof, Centrifugal and Axial Flow Pumps, John Wiley & Sons, Inc., New York., 2nd Edition, 1957, pp. 116-123.

3. H.J. Biheller, Radial Force on the Impeller of Centrifugal Pumps With Volute, Semivolute, and Fully Concentric Casings, ASME, Journal of Engineering for Power, Vol. 87, July, 1965, pp. 319-3123.

Fig. 1- Cross section of expander-compressor with magnetic bearings

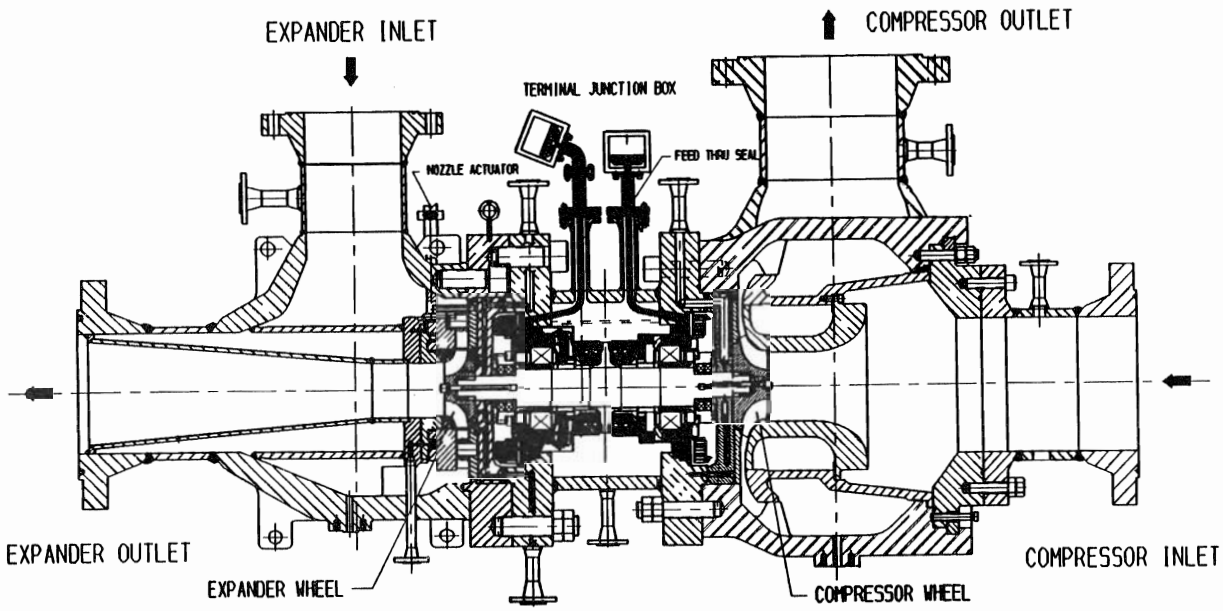

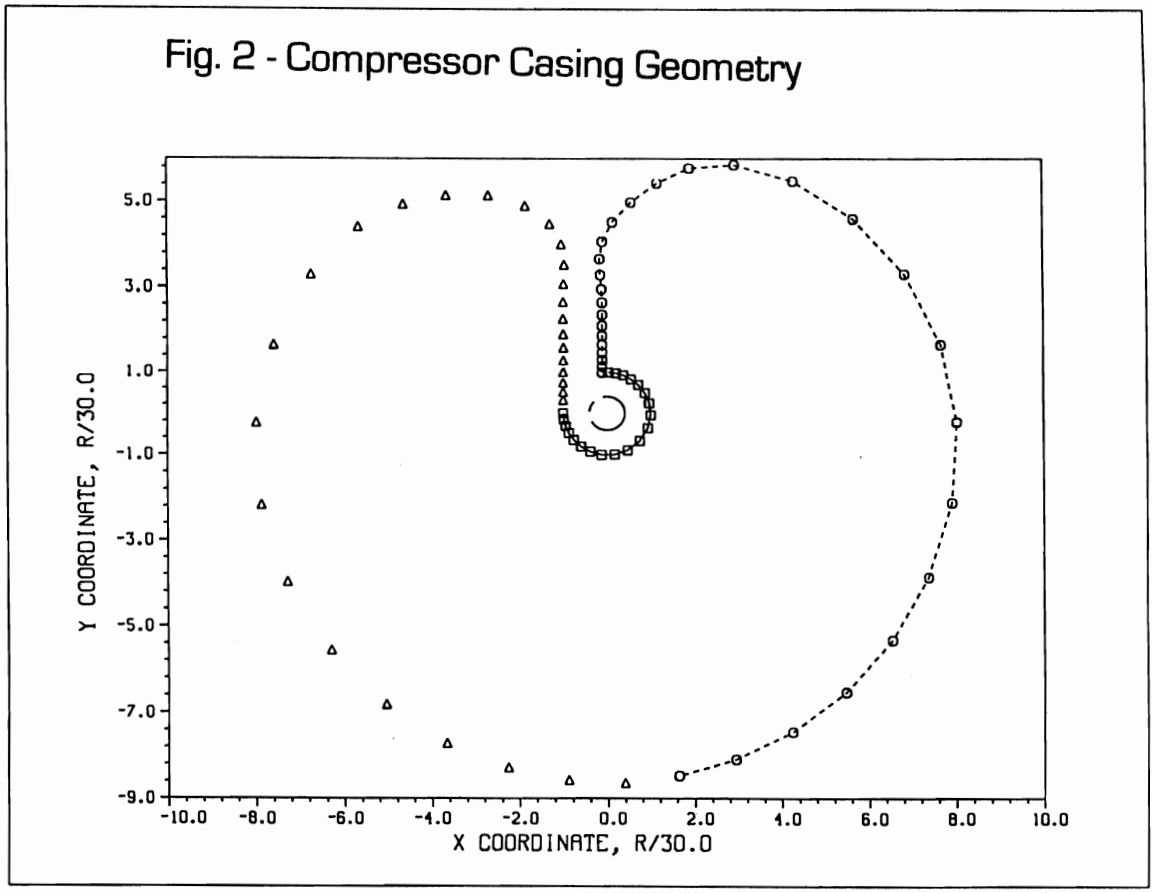

Fig. 3 - Transformed Compressor Casing Geometry

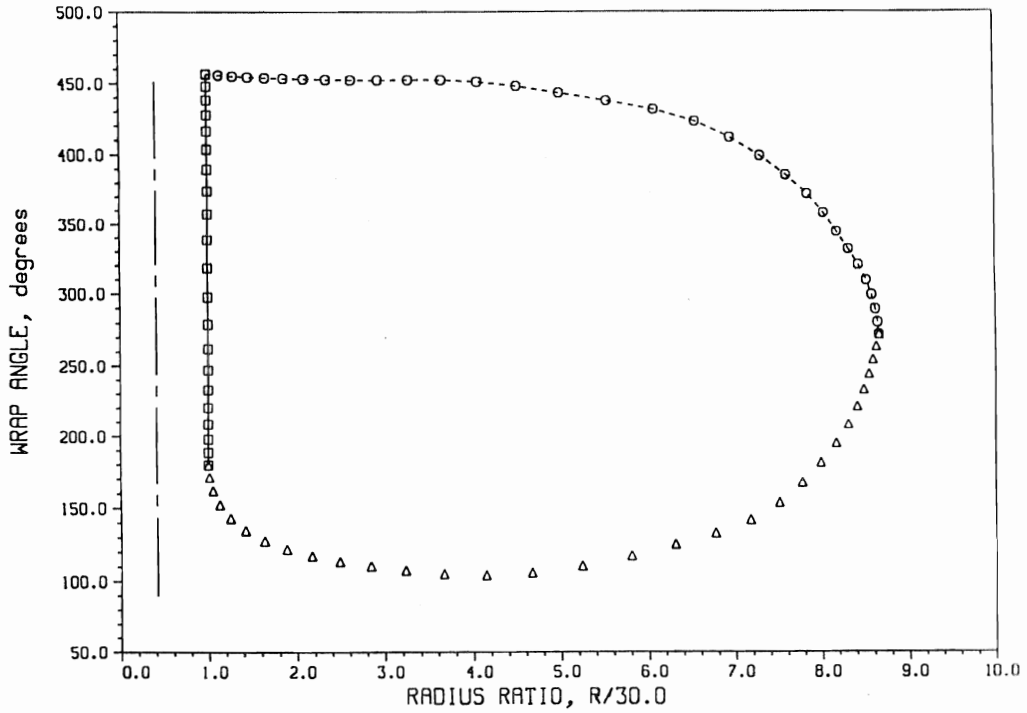

Fig. 4 - Cascade Simulation for Compressor Casing

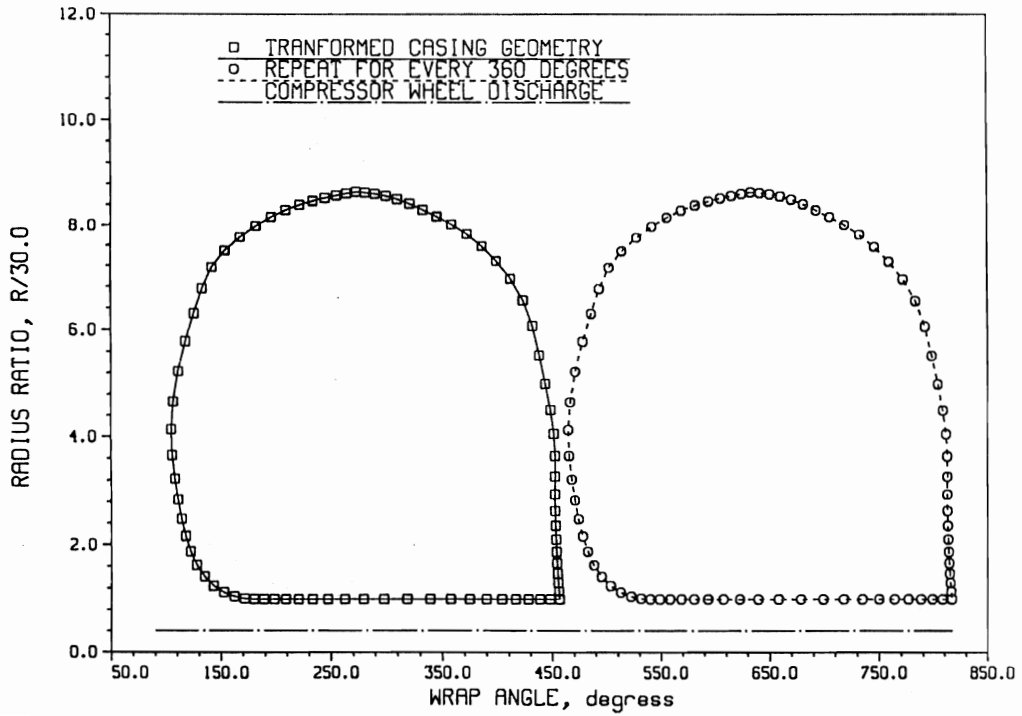

Fig. 5 - Equivalent Cascade Streamtube Thickness Distribution

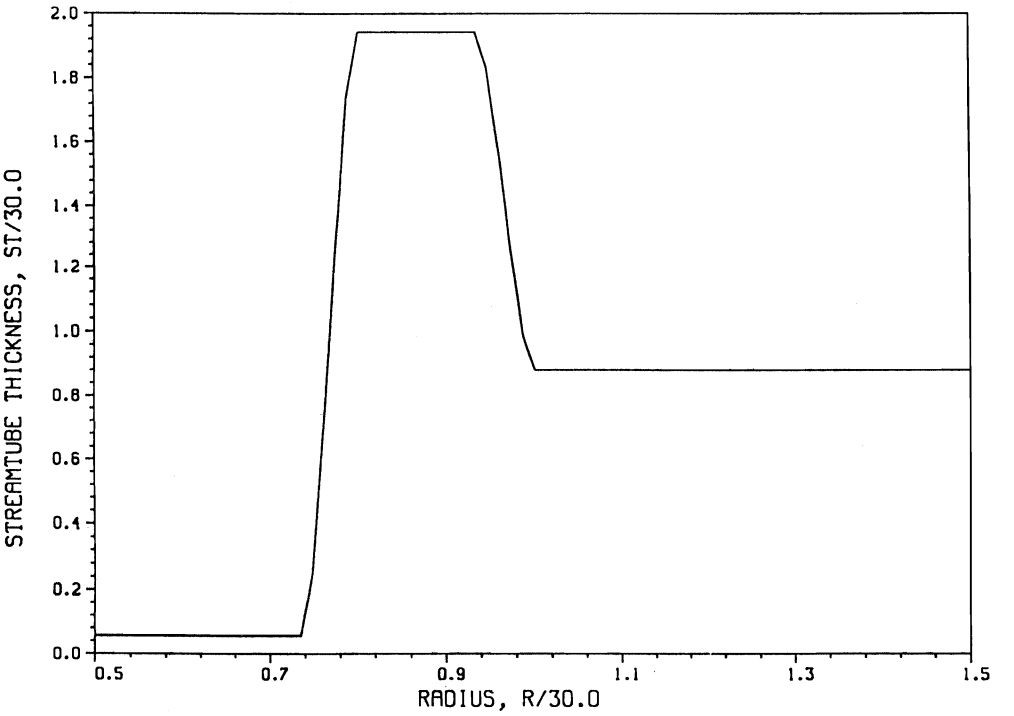

Fig. 6 - Compressor Wheel Discharge Radial Velocity

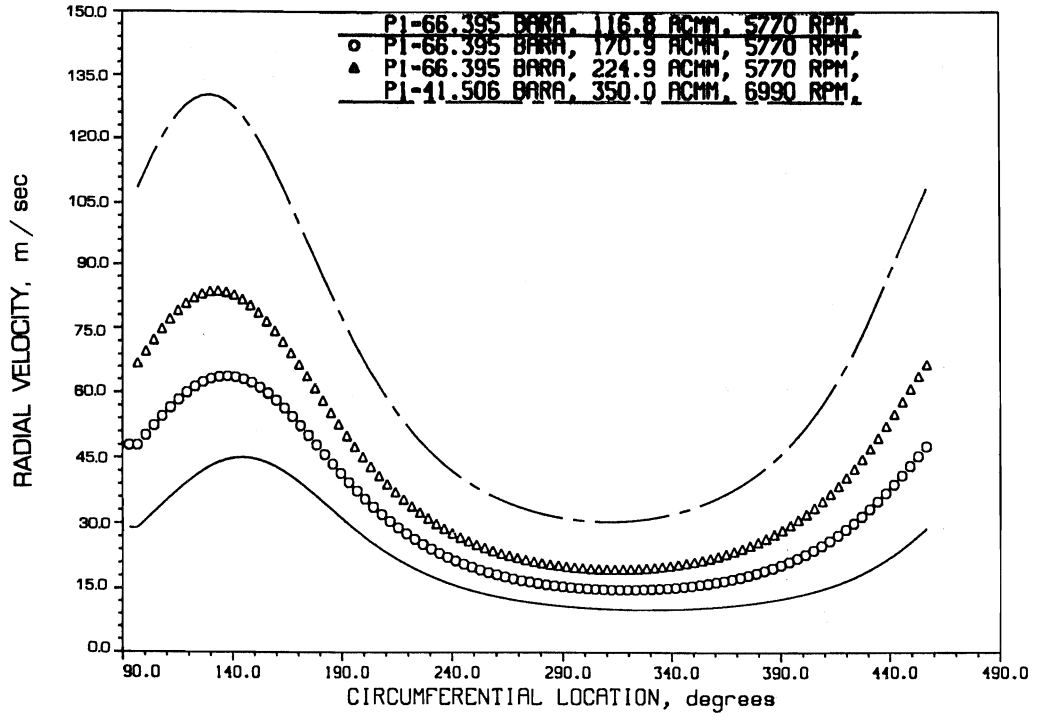

Fig. 7 - Compressor Wheel Discharge Total Velocity

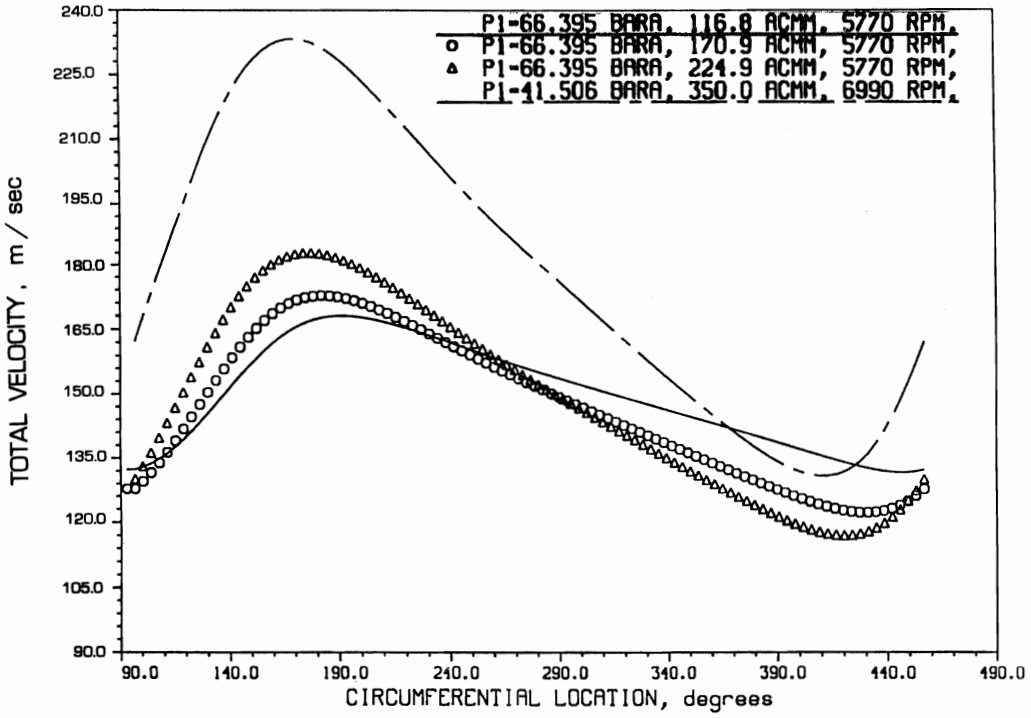

Fig. 8 - Wheel Discharge Static Pressure Rise

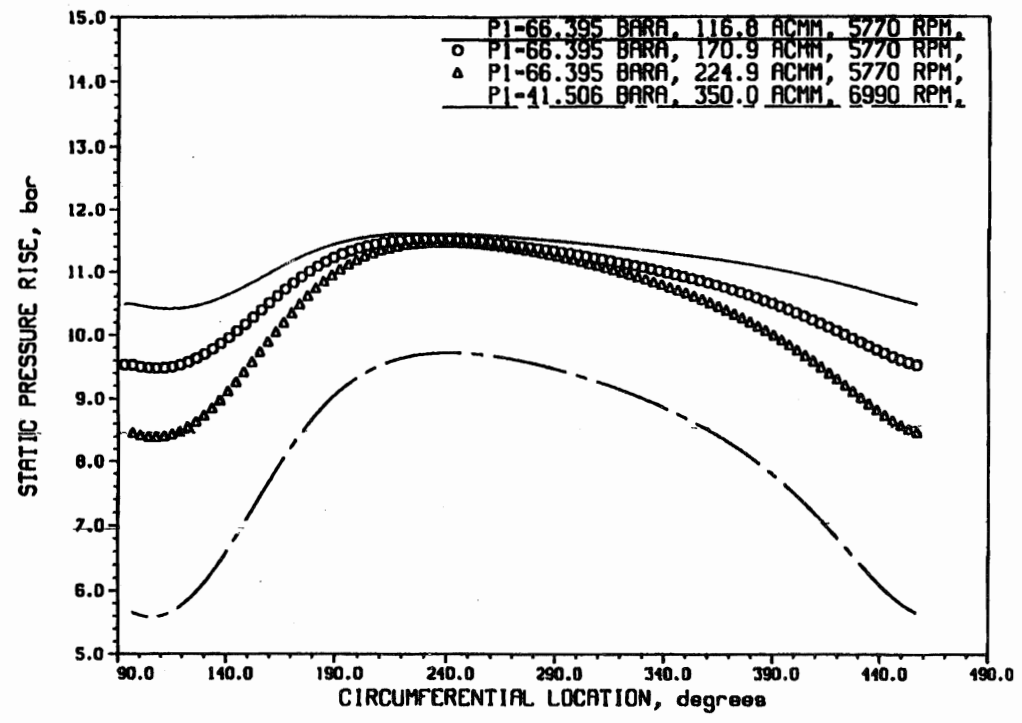

Fig. 9 - Radial Thrust and Flow Relationship

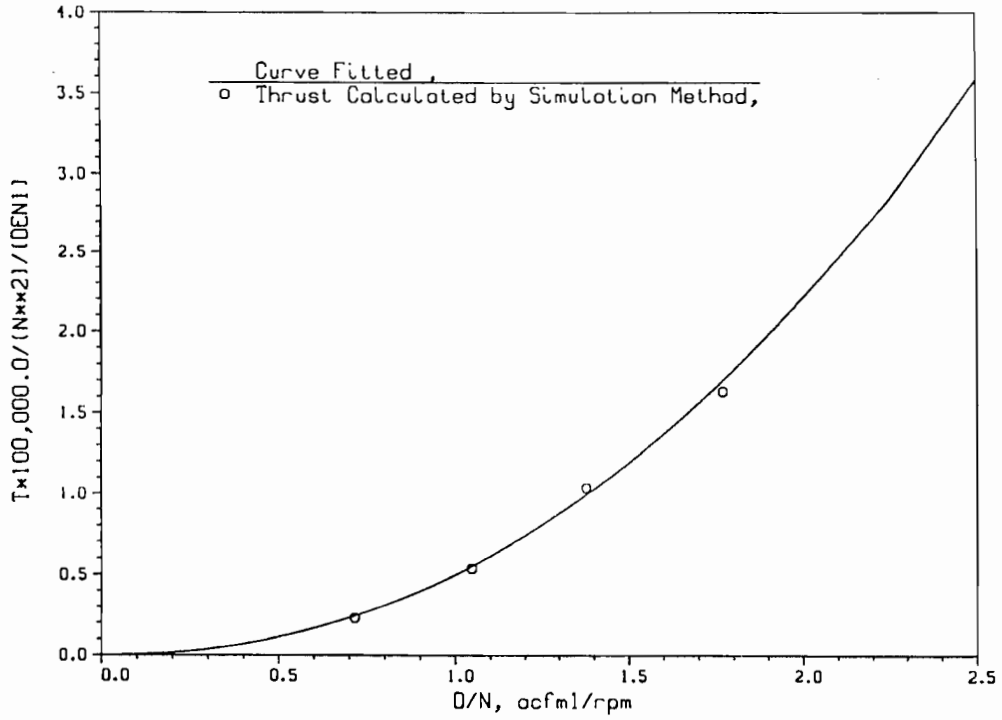

Fig. 10 - Radial Thrust Direction Prediction

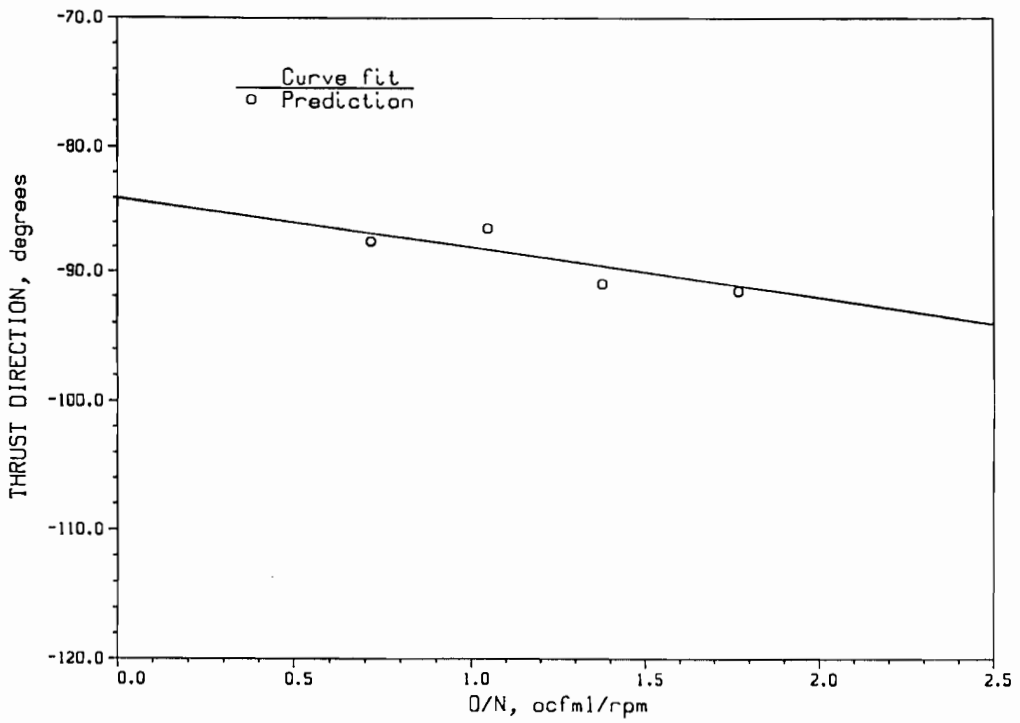

Fig. 11 - Radial Thrust Prediction

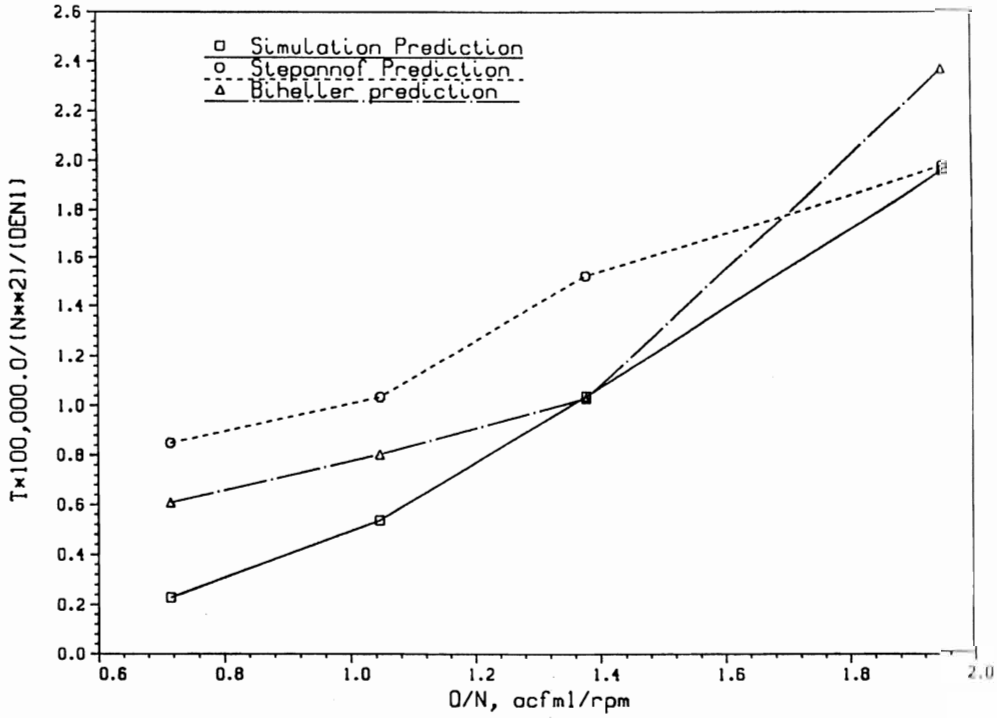

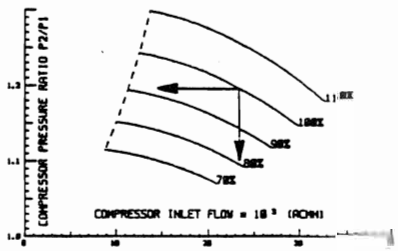

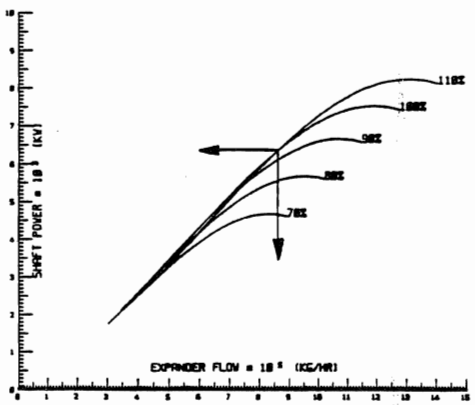

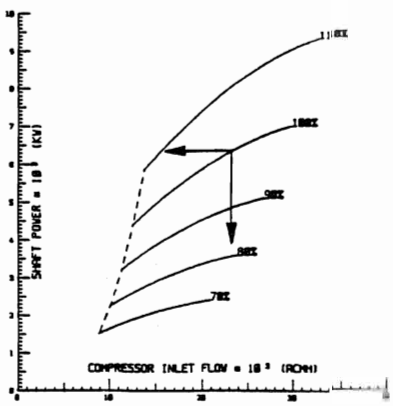

Table I. Gas dynamics radial force

TYPE OF RADIAL THRUST	7943 ACFM AT 5770 RPM	13633 ACFM AT 6990 RPM
MAXIMUM	664 KILOGRAMS	1328 KILOGRAMS
MEAN	419 KILOGRAMS	693 KILOGRAMS
MINIMUM	220 KILOGRAMS	280 KILOGRAMS